

PHYSICAL REVIEW D **66**, 034029 (2002)**Diffractive effects in spin-flip  $pp$  amplitudes and predictions for relativistic energies**

A. F. Martini\*

*Instituto de Física Gleb Wataghin, Universidade Estadual de Campinas,  
Unicamp, 13083-970 Campinas, São Paulo, Brazil*

E. Predazzi†

*Università di Torino and INFN, Sezione di Torino,  
Via Pietro Giuria, 1, 10125 Torino, Italy*

We analyze the diffractive (Pomeron) contribution to  $pp$  spin-flip amplitude and discuss the possible scenarios for energies available at the Relativistic Heavy-Ion Collider (RHIC). In particular, we show that RHIC data will be instrumental in assessing the real contribution of diffraction to spin amplitudes.

PACS numbers: 13.88.+e, 11.55.Jy, 25.40.Cm

**I. INTRODUCTION**

The study of diffraction on high-energy scattering using Regge formalism is a well-known subject [1]. Until the coming in operation of Relativistic Heavy-Ion Collider (RHIC), the highest energy  $pp$  data available from accelerators were those of the Intersecting Storage Ring (ISR) at CERN. Those experiments, however, did not measure the polarization of the projectiles. Since the differential cross section ( $d\sigma/dt$ ) at ISR energies is usually assumed to be dominated by the spin-non-flip amplitude, many of the models describing the diffraction in  $pp$  scattering do not take into account the contribution from spin-flip amplitudes [2, 3, 4]. Others do [5, 6, 7, 8] but in this case they use data at lower energies [9]. However, the study of diffraction in spin-flip amplitudes began many years before that when one of us [10] noticed that polarization data at  $\pi p$  scattering suggested a diffractive contribution in the spin-flip  $\pi p$  amplitude at high energy which becomes evident when the kinematical zero is removed. The spin-flip amplitude without the kinematical zero is named “reduced” and manifests itself as a peak in the forward direction which does not appear to vanish as the energy increases. In Ref. [10] it was explicitly noticed that, once the kinematical zero is removed, all partial waves act coherently in the small angle domain as it is typical of diffractive events [11]. The following statement was made later [12]: “*the residual spin-flip amplitudes behave very much like spin-non-flip amplitudes at high energies and exhibit a pronounced forward peak which is largely independent of the particular elastic reaction chosen*”. The same conclusion was obtained in the analysis of  $pp$  data some years later [12] but in the case of  $pp$  scattering the situation is complicated by the existence of five independent helicity amplitudes, named  $\phi_j$ , with  $j = 1, \dots, 5$ . Of those,  $\phi_1$  and  $\phi_3$  are spin-non-flip amplitudes,  $\phi_2$  and  $\phi_4$  are double spin-flip amplitudes, and  $\phi_5$  is a single spin-flip amplitude.

In this work we are interested in high energy and not too high  $t$  so that we can concentrate the analysis on the main aspects of the spin-flip amplitude for  $pp$  scattering in the diffractive region. In Ref. [7] the magnitudes of  $\phi_2$  and  $\phi_4$  with respect to the spin-non-flip amplitude were analyzed and reasonable arguments were given concerning the linear dependence on  $t$  for  $\phi_2$  ( $\phi_2 \propto t$  when  $t \rightarrow 0$ ) [15], while in the case of  $\phi_4$  the relation  $\phi_4 \propto t$  is consequence of angular momentum conservation.

So, the general form of the polarization  $P$  for  $pp$  scattering

$$P = 2 \frac{\text{Im}[(\phi_1 + \phi_2 + \phi_3 - \phi_4)\phi_5^*]}{[|\phi_1|^2 + |\phi_2|^2 + |\phi_3|^2 + |\phi_4|^2 + 4|\phi_5|^2]} \quad (1)$$

can be simplified assuming that  $\phi_2$  and  $\phi_4$  are small compared to the others amplitudes in the  $t$  region under interest. Using the definitions

$$\phi_1 = \frac{g(s, t)}{2}, \quad \phi_5 = \frac{h(s, t)}{2}, \quad (2)$$

\*Electronic address: martini@if.unicamp.br

†Electronic address: predazzi@to.infn.it

where  $g(s, t)$  and  $h(s, t)$  will be considered *effective* spin-non-flip and spin-flip amplitudes, respectively, and assuming  $\phi_1 = \phi_3$  the polarization can be rewritten as

$$P = 2 \frac{\text{Im}[g(s, t)h^*(s, t)]}{|g(s, t)|^2 + 2|h(s, t)|^2}. \quad (3)$$

Today, a rather considerable amount of data at higher energies has been gathered [9] in the relatively small angle domain and new perspectives are being opened by the coming in operation of the Relativistic Heavy Ion Collider (RHIC), the ideal machine to study polarization in high energy collision processes [13].

In addition, our phenomenological information on the spin-non-flip amplitude is today much more complete and this can be used to reduce the uncertainties in the analysis. Using an explicit parametrization for the  $pp$  spin-non-flip amplitude [14] whose parameters have been calculated against all high energy  $pp$  and  $\bar{p}p$  data (except polarization), we analyze the structure of the reduced spin-flip contribution, where the kinematical zero is removed with the factor  $\sqrt{-t}$ . The following conclusions are reached in this analysis.

(a) The (reduced) spin-flip amplitude exhibits the typical peak in the forward direction which characterizes diffractive amplitudes but the reduced spin-flip amplitude is less than 10% of the imaginary part of the spin-non-flip amplitude. (b) The data fitting with the same energy dependence in  $g(s, t)$  and  $h(s, t)$  seems the best choice; a zero is automatically produced in the polarization; this moves with energy towards  $t = 0$  as a consequence of the analogous shift of the dip in  $d\sigma/dt$  induced by the zero of the spin-non-flip amplitude. (c) The magnitude of the polarization decreases as the energy increases but the extrapolation to 500 GeV predicts a non-negligible contribution if the same Pomeron trajectory for both spin-flip and spin-non-flip amplitudes is used.

In the next section we present the expressions of the amplitudes and explain them. In Sec. III we show the fit of the data and the modifications on the spin-flip amplitudes. We also consider a similar (nondiffractive) analysis of the data. Although the fit to the lower energy data is essentially the same, the two analysis predict a very different behavior at increasing energies. As we will stress, RHIC data should provide a reasonably clear cut answer to the question of whether or not diffraction contributes to the spin-flip amplitude. In Sec. IV we present the conclusions.

## II. DEFINITION OF THE AMPLITUDES

The *effective*  $pp$  spin-non-flip amplitude will be written as

$$g(s, t) = a^{nf}(s, t) = a_+(s, t) - a_-(s, t) \quad (4)$$

with

$$a_+(s, t) = a_P(s, t) + a_f(s, t) \quad \text{and} \quad a_-(s, t) = a_O(s, t) + a_\omega(s, t), \quad (5)$$

where  $a_P(s, t)$  and  $a_O(s, t)$  are the Pomeron and Odderon amplitudes, respectively, and  $a_f(s, t)$  [ $a_\omega(s, t)$ ] is the even (odd) secondary Reggeon [16]. These different amplitudes are taken directly from Ref. [14] and their explicit forms are given in the Appendix together with the values of their parameters.

To write the effective spin-flip amplitude  $h(s, t)$ : (i) first, we neglect the spin contribution of secondary Reggeons to check whether diffraction could be the dominant phenomenon for the spin-flip amplitude at small  $|t|$  at the available energies; (ii) second, we notice that the combination of the exchange of two and three gluon ladders induce  $CP$ -even (and -odd) contributions to the spin-flip amplitude that affects Pomeron exchange. We have, therefore, to anticipate that the diffractive (Pomeron) contribution to the spin-flip amplitude may have a slightly modified structure from the usual one. Differently stated, to take into account three gluon ladders, we do not take a strict Regge pole parametrization for the Pomeron spin-flip term and we allow a real part contribution to be present. Thus, in the very small  $|t|$  domain, we write

$$\begin{aligned} h(s, t) = a^{sf}(s, t) &= (i\gamma_1 + \delta_1) \frac{\sqrt{-t}}{m_p} \tilde{s}^{\alpha^{sf}(t)} e^{\beta_1 t} \Theta(0.5 - |t|) \\ &+ (i\gamma_2 + \delta_2) \frac{\sqrt{-t}}{m_p} \tilde{s}^{\alpha^{sf}(t)} e^{\beta_2 t} \Theta(|t| - 0.5), \end{aligned} \quad (6)$$

where the mass of the proton  $m_p$  is used to make the parameters dimensionless. In Eq. (6)  $\tilde{s} = (s/s_0)e^{-i\pi/2}$ ,  $\Theta$  is the step function and we assume  $s_0 = 1 \text{ GeV}^2$  as in Ref. [14]; the superscript  $sf$  (for “spin-flip”) allows us to check if the  $P$  trajectory can be different for spin-flip and spin-non-flip amplitudes. While the complex phase in Eq. (6) is used to take into account in a phenomenological way the mixing of  $CP$  even and odd contributions cited above, the step

function is used to account in the most economical way for the fact that the fitting procedure requires a change in the slope of  $h(s, t)$  (similar to what happens in  $d\sigma/dt$ ) to have a good description of the polarization data. The precise point where the slope changes, however, is rather  $t$  insensitive and could be taken at almost any value between 0.2 and 0.7 GeV<sup>2</sup> (in  $|t|$ ). We do not have an explanation for this effect nor for the insensitivity in the choice of the point where the slope changes but it proves that our parametrization is quite stable. To start with, we take the spin-flip Pomeron trajectory  $\alpha^{sf}(t)$  to be exactly the same as derived for the spin-non-flip amplitude

$$\alpha^{sf}(t) = \alpha_{\mathcal{P}}(t) = \alpha_{\mathcal{P}}(0) + \alpha'_{\mathcal{P}}t, \quad (7)$$

where  $\alpha_{\mathcal{P}}(0)$  and  $\alpha'_{\mathcal{P}}$  are given in the Appendix .

### III. FIT TO THE EXISTING $pp$ POLARIZATION DATA

The differential cross section  $d\sigma/dt$  for  $pp$  scattering is available at energies up to 63 GeV in the c.m. system but polarization data are available only at lower energies. We utilized the data at  $\sqrt{s} = 13.8, 16.8, \text{ and } 23.8$  GeV (a total of 64 points) in the fit and we checked the quality of the result describing the polarization at 19.4 GeV. The parameters obtained in the fit are shown in Table I with the best  $\chi^2$  per degree of freedom. In principle (and in practice), the inclusion of the spin-flip amplitude in the game would require refitting all the parameters to reproduce the angular distributions as well. We will check, however, that the fit of the polarization data *without* performing a new fit to the angular distribution does not modify the quality of the fit to the latter while making much more direct the analysis of the polarization data

Figure 1 presents the set of polarization data used in the fit together with our reconstruction. Figure 2 shows the polarization at  $\sqrt{s} = 19.4$  GeV with the prediction of our model since this set was not used in the fit. In Fig. 3 we show  $d\sigma/dt$  at various energies as described by adding the (squared) spin-flip amplitude [see Eq. (A.9) in the Appendix ] to the (squared) spin non flip term. As anticipated, the quality of the fit has not been altered.

Several comments are in order.

(a) The  $\mathcal{P}$  contribution to the spin-flip amplitude  $h(s, t)$  is considerably smaller than to the spin-non-flip term  $g(s, t)$  (about 5%, roughly, at  $\sqrt{s} = 20$  GeV and changing little until 500 GeV). This value is compatible with the analysis performed in [7] where use was made of the relative amplitude  $r_5 = m\phi_5/(\sqrt{-t} \text{Im}\phi_+)$ . In our case,  $\text{Im} r_5 = -0.054$  at  $\sqrt{s} = 500$  GeV. We should mention that we find *natural* that the spin-flip part of the amplitude should be a small fraction of the spin-non-flip but, again, we have no real reason for this. (b) Contrary to the discussion made in Ref. [12], the (small  $|t|$ ) slope of the spin-flip amplitude  $\beta_1 = 4.74 \text{ GeV}^{-2}$  appears to be not very much different from the effective slope of the Pomeron in spin-non-flip amplitude (see the Appendix ). The present parametrization, however, is considerably more elaborate and the set of data corresponds to higher energies so the results of these papers may not be directly comparable. (c) Our result [i.e.,  $h(s, t)$ ] cannot be extended to  $|t|$  values much higher than few GeV<sup>2</sup> because the spin-non-flip amplitude utilized is valid at the Born level [14] and its description in the region after the dip ( $|t| > 1.5 \text{ GeV}^2$ ) is not very good. To extend our considerations to higher  $|t|$ , it would be necessary to adopt the more sophisticated eikonized version. Anyway, the  $t$  region of interest for RHIC is up to 1.5 GeV<sup>2</sup> [13] so we can confine our analysis to the not too high  $|t|$  region. This point may have to be reconsidered in the future along with more detailed analysis. (d) The spin-non-flip amplitude in Ref. [14] fits  $d\sigma/dt$  without the spin contribution and that description is not spoiled by the presence of  $h(s, t)$  on this work since it is very smaller than  $g(s, t)$ .

#### A. The kinematical zero of the spin-flip amplitude

The original work about diffraction and polarization data at  $\pi p$  scattering calculated the reduced spin-flip amplitude removing the kinematical zero by means of a  $\sin \theta$  instead of  $\sqrt{-t}$  [10]. Since the energies available at that time were much lower, it would be difficult to see differences between the two approaches. But the data presently available and the coming in operation of RHIC at even higher energies raises the question of what would happen if the factor  $\sin \theta$  was used. In principle, the use of relativistically invariant variables used earlier seems more appropriate but we feel that the answer can only come from experiments.

To answer this question we adopt in this section the spin-flip amplitude

$$\begin{aligned} h(s, t) = a^{sf}(s, t) = & (i\gamma_1 + \delta_1) \sin \theta \tilde{s}^{\alpha^{sf}(t)} e^{\beta_1 t} \Theta(0.5 - |t|) \\ & + (i\gamma_2 + \delta_2) \sin \theta \tilde{s}^{\alpha^{sf}(t)} e^{\beta_2 t} \Theta(|t| - 0.5). \end{aligned} \quad (8)$$

We use the same procedure of the fit with Eq. (6), that is, we fit the data at  $\sqrt{s} = 13.8, 16.8$  and  $23.8$  GeV assuming  $\alpha^{sf}(t) = \alpha_P(t)$ . Then we check the quality of the fit with the description of the polarization data at  $19.4$  GeV. The values of the parameters obtained with Eq. (8) are shown in Table II.

Following the same procedure of the previous section, we present in Fig. 4 the result of the fitting while Fig. 5 shows the polarization at  $\sqrt{s} = 19.4$  GeV and Fig. 6 presents  $d\sigma/dt$ . Two differences in the present results and in those of the previous analysis are worth being emphasized. First, the ratio of the reduced spin-flip  $[h(s, t)/\sin\theta]$  to the spin-non-flip amplitude is much bigger (above 90%) and this big ratio was noticed at lower energies too [12]. Second, the slope  $\beta_1 = 6.25$  GeV<sup>2</sup> is higher than the previous result (Table I) so the reduced spin-flip amplitude is steeper on this case.

Although Eqs. (6) and (8) present very different values for the parameters  $\beta_1$ ,  $\delta_1$ , and  $\gamma_1$ , Figs. 1-6 show that the descriptions of the data are similar and the fits have a comparable  $\chi^2$ . To understand the consequences of using one parametrization or the other it is necessary to remember that  $\sin\theta \propto \sqrt{-t/s}$ . So, to all effects, Eq. (8) does not have the  $s$  dependence of the Pomeron. Differently stated, the parametrization (8), ultimately, is not diffractive. The comparison between the two parametrizations used for  $h(s, t)$ , therefore, Eqs. (6) and (8) goes to the root of the problem of whether or not diffraction contributed to spin-flip. This difference will have relevant consequences at higher energies and the  $pp2pp$  experiment at RHIC [13] will be able to discriminate between these two scenarios.

## B. Predictions to higher energies

The  $pp2pp$  experiment at RHIC will provide information about polarization in  $pp$  scattering at energies between 50 and 500 GeV [13]. That means a big increase in the amount of information about the spin content of the proton so it is important to see what we can say about the polarization in that energy range based on the information we have derived from the data available at lower energies. To this aim, we calculate the polarization at  $\sqrt{s} = 50$  and 500 GeV with Eq. (6) plotting the result in Fig. 7. We can see that the polarization decreases in magnitude with increasing energy but it is still sizeable at 500 GeV. Equation (6) produces a peak of about 10% of positive polarization around  $-t = 1.25$  GeV<sup>2</sup> and  $\sqrt{s} = 500$  GeV as compared with a (positive) polarization of over 15% at  $\sqrt{s} = 50$  GeV.

Now we compare this result with the prediction using Eq. (8) (see Fig. 8). The polarization calculated with the factor  $\sin\theta$  is much smaller (about 5% at  $\sqrt{s} = 50$  GeV) but becomes essentially zero at  $\sqrt{s} = 500$  GeV. As already mentioned the factor  $1/\sqrt{s}$  hidden inside the sine function is important to separate the predictions at high energies.

We have also checked the possibility of a different intercept for the trajectory  $\alpha^{sf}(t)$ . In this case Eq. (7) is modified and  $\alpha^{sf}(0)$  becomes a new parameter to be fitted together with the other six parameters. The values obtained (with a similar  $\chi^2/N_{DF}$ ) for them were quite absurd, including a negative intercept  $\alpha^{sf}(0)$  when the factor  $\sqrt{-t}/m_p$  is used, and the polarization predictions at RHIC energies are so small that it would be essentially impossible to detect those values experimentally. Since there is no improvement of the fit with the increased number of parameters we discard this solution.

## IV. CONCLUSIONS

We analyzed the spin-flip amplitude and removed its kinematical zero to study the Pomeron contribution to the spin as suggested long time ago [10, 12]. We made use of two hypothesis to remove the zero,  $\sqrt{-t}/m_p$  and  $\sin\theta$ , where the first is more convenient at high energies since it is relativistic invariant while the second was used in the original work about diffraction in  $pp$  spin-flip amplitudes [12]. The differences resulting from the application of Eqs. (6) or (8) are quite large although the descriptions of the data between  $\sqrt{s} = 13$  and 24 GeV are very similar. The fraction of  $h(s, t)$  to  $g(s, t)$  is small if  $\sqrt{-t}/m_p$  is used (around 5%) but it becomes big when  $\sin\theta$  is utilized (more than 90%). Although, as already mentioned, we do not have a strict reason to prefer one over the other, the first solution is much more in line with the traditional analyses. Also, the slope at small  $|t|$  changes when  $\sqrt{-t}/m_p$  is substituted by  $\sin\theta$ , showing that  $h(s, t)$  becomes steeper with the second option. At the same time, the slope  $\beta_2$  is practically the same in both cases showing that there is a modification on  $h(s, t)$  around  $-t = 0.5$  GeV<sup>2</sup>, which confirms the necessity of two slopes in the spin-flip amplitude as it was assumed. The extrapolations shown in Figs. 7 and 8 suggest that the data from RHIC will be crucial to understand and choose the best form to describe the spin-flip amplitude.

In summary, the prediction is very straightforward: a positive polarization of the order of 10% is predicted at RHIC energies of  $\sqrt{s} = 500$  GeV if the Pomeron (diffraction) contributes to the spin-flip amplitude as lower energy data tend to suggest. A vanishing contribution is otherwise expected.

It would be possible to improve the description of the data with more elaborated forms for both spin-non-flip and spin-flip amplitudes (by eikonizing them, for example, Ref. [14], by introducing subasymptotic effects in the spin-flip part by secondary Reggeons and so on) but we expect that the main conclusions of our analysis would remain the same

in the region of small  $t$  (where the Born amplitudes work well) and high energies (where the Pomeron dominates). A more detailed analysis to separate the contributions of the exchanges of two and three gluon ladders would be more gratifying from the theoretical point of view as well as a better study of the break in the diffractive slopes. All these points will, hopefully, be reconsidered in the future.

### Acknowledgments

Several discussions with Professor E. Martynov and Professor M. Giffon and the comments and suggestions of Professor O. V. Selyugin are gratefully acknowledged. Work supported in part by the MURST of Italy. One of us (A.F.M.) would like to thank the Department of Theoretical Physics of the University of Torino for its hospitality and the FAPESP of Brazil for its financial support.

### APPENDIX: THE SPIN-NON-FLIP AMPLITUDE

The spin-non-flip amplitude utilized in this work is

$$a^{nf}(s, t) \equiv a_+(s, t) - a_-(s, t), \quad (\text{A.1})$$

where

$$a_+(s, t) = a_P(s, t) + a_f(s, t) \quad (\text{A.2})$$

and

$$a_-(s, t) = a_O(s, t) + a_\omega(s, t). \quad (\text{A.3})$$

The expressions for the two Reggeons used in Ref. [14] are

$$a_R(s, t) = a_R \tilde{s}^{\alpha_R(t)} e^{b_R t} \quad (\text{A.4})$$

and

$$\alpha_R(t) = \alpha_R(0) + \alpha'_R t \quad (R = f \text{ and } \omega) \quad (\text{A.5})$$

with  $a_f(a_\omega)$  real (imaginary).

For the Pomeron, the spin-non-flip amplitude is

$$a_P^{(D)}(s, t) = a_P \tilde{s}^{\alpha_P(t)} [e^{b_P[\alpha_P(t)-1]}(b_P + \ln \tilde{s}) + d_P \ln \tilde{s}] \quad (\text{A.6})$$

while for the Odderon we use

$$a_O(s, t) = [1 - \exp(\gamma t)] a_O \tilde{s}^{\alpha_O(t)} [e^{b_O(\alpha_O(t)-1)}(b_O + \ln \tilde{s}) + d_O \ln \tilde{s}], \quad (\text{A.7})$$

where again  $a_P(a_O)$  real (imaginary) and we have utilized  $\alpha_i(t) = \alpha_i(0) + \alpha'_i t$ , where  $i = P, O$ .

Our definition for the amplitude follows [14] so that

$$\sigma_t = \frac{4\pi}{s} \text{Im}\{a^{nf}(s, t=0)\}, \quad (\text{A.8})$$

$$\frac{d\sigma}{dt} = \frac{\pi}{s^2} [|a^{nf}(s, t)|^2 + 2|a^{sf}(s, t)|^2]. \quad (\text{A.9})$$

In this work we retain the same parameters for the spin-non-flip amplitude as in Ref. [14] and we keep them fixed while fitting the parameters of the spin-flip amplitude. We utilize the dipole model at the Born level since most of the polarization data is contained in the  $t$  domain corresponding to the region before the dip in  $d\sigma/dt$  (well described without eikonalization). The values of the parameters of the spin-non-flip amplitude [14] are shown in Table III.

To calculate the polarization we utilized the form

$$P = 2 \frac{\text{Im}\{a^{nf}(s, t)[a^{sf}(s, t)]^*\}}{|a^{nf}(s, t)|^2 + 2|a^{sf}(s, t)|^2}, \quad (\text{A.10})$$

where the star on the numerator means complex conjugate.

- 
- [1] E. Predazzi, in *Proceedings of the International Workshop on Hadron Physics 98*, edited by E. Ferreira, F. F. de Souza Cruz, and S. S. Avancini (World Scientific, Singapore, 1999), p. 80; see also V. Barone and E. Predazzi, *High Energy Particle Diffraction* (Springer-Verlag, Berlin, 2002).
- [2] P. Desgrolard, M. Giffon, and E. Martynov, *Eur. Phys. J. C* **18**, 359 (2000).
- [3] P. Desgrolard, M. Giffon, and E. Predazzi, *Z. Phys. C* **63**, 241 (1994).
- [4] A. Donnachie and P. V. Landshoff, *Nucl. Phys.* **B231**, 189 (1984).
- [5] C. Bourrely, J. Soffer, and Tai Tsun Wu, *Phys. Rev. D* **19**, 3249 (1979).
- [6] S. V. Goloskokov, S. P. Kuleshov, and O. V. Selyugin, *Z. Phys. C* **50**, 455 (1991).
- [7] N. H. Buttmore *et al.*, *Phys. Rev. D* **59**, 114010 (1999).
- [8] N. Akchurin, S. V. Goloskokov, and O. V. Selyugin, *Int. J. Mod. Phys. A* **14**, 253 (1999).
- [9] R. V. Kline *et al.*, *Phys. Rev. D* **22**, 553 (1980); G. Fidecaro *et al.*, *Nucl. Phys.* **B173**, 513 (1980); G. Fidecaro *et al.*, *Phys. Lett. B* **105**, 309 (1981); J. Snyder *et al.*, *Phys. Rev. Lett.* **41**, 781 (1978).
- [10] E. Predazzi and G. Soliani, *Nuovo Cimento A* **51**, 427 (1967).
- [11] M. L. Good and W. D. Walker, *Phys. Rev.* **120**, 1857 (1960).
- [12] K. Hinotani, H. A. Neal, E. Predazzi, and G. Walters, *Nuovo Cimento A* **52**, 363 (1979).
- [13] W. Guryin, *Nucl. Phys. B (Proc. Suppl.)* **99**, 299 (2001).
- [14] P. Desgrolard, M. Giffon, E. Martynov, and E. Predazzi, *Eur. Phys. J. C* **16**, 499 (2000).
- [15] A similar dependence was also utilized in another work where the impact parameter space was used [6].
- [16] Actually,  $a_f$  embodies both  $f$  and  $\rho$  contributions (and  $a_\omega$  both  $\omega$  and  $a_2$ ).

TABLE I: Values of the parameters obtained from fitting polarization data at  $\sqrt{s} = 13.8, 16.8, \text{ and } 23.8$  GeV with Eqs. (6) and (7). The  $\chi^2/N_{\text{DF}}$  is 1.1.

i	$\gamma_i$	$\delta_i$	$\beta_i$ (GeV $^{-2}$ )
1	$1.35 \times 10^{-1}$	$2.64 \times 10^{-1}$	4.74
2	$2.55 \times 10^{-2}$	$5.38 \times 10^{-2}$	2.29

TABLE II: Results from fitting polarization data at  $\sqrt{s} = 13.8, 16.8, \text{ and } 23.8$  GeV with Eqs. (7) and (8). The  $\chi^2/N_{\text{DF}}$  is 1.1.

i	$\gamma_i$	$\delta_i$	$\beta_i$ (GeV $^{-2}$ )
1	2.55	4.80	6.25
2	0.18	0.45	2.30

TABLE III: Parameters of the dipole model at the Born level [14] with  $i = P, O, f, \omega$ .

	Pomeron	Odderon	$f$ Reggeon	$\omega$ Reggeon
$\alpha_i(0)$	1.071	1.0	0.72	0.46
$\alpha'_i$ (GeV $^{-2}$ )	0.28	0.12	0.50	0.50
$a_i$	-0.066	0.100	-14.0	9.0
$b_i$	14.56	28.10	1.64 GeV $^{-2}$	0.38 GeV $^{-2}$
$d_i$	0.07	-0.06	-	-
$\gamma$ (GeV $^{-2}$ )	-	1.56	-	-

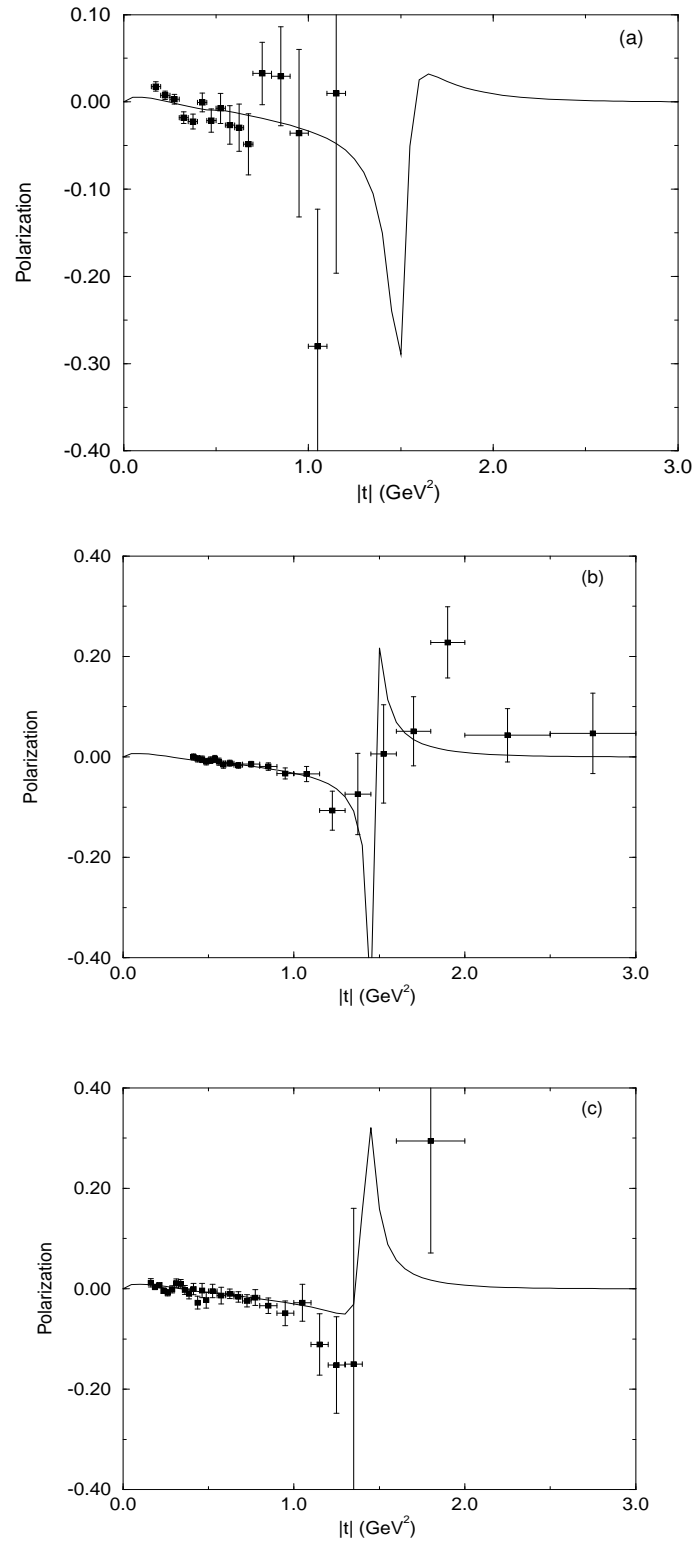


FIG. 1: Results from fitting polarization data at (a) 13.8 GeV, (b) 16.8 GeV, and (c) 23.8 GeV (see Table I).

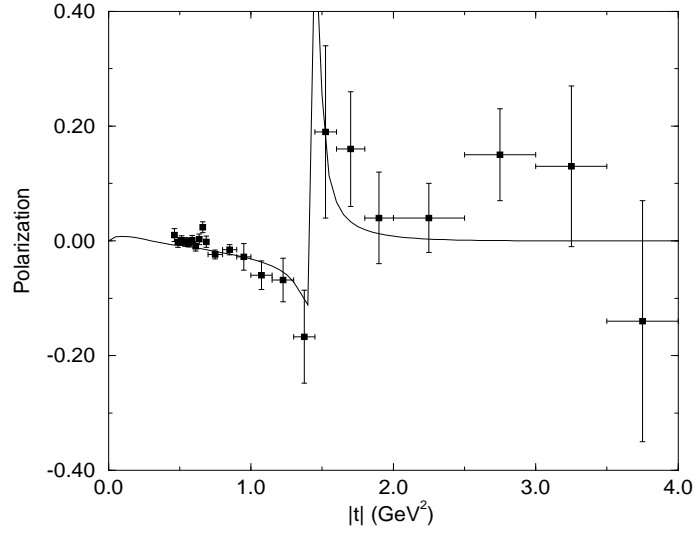


FIG. 2: The prediction for the polarization at 19.4 GeV (not used in the fit) compared with the experimental data at that energy (parameters from Table I).

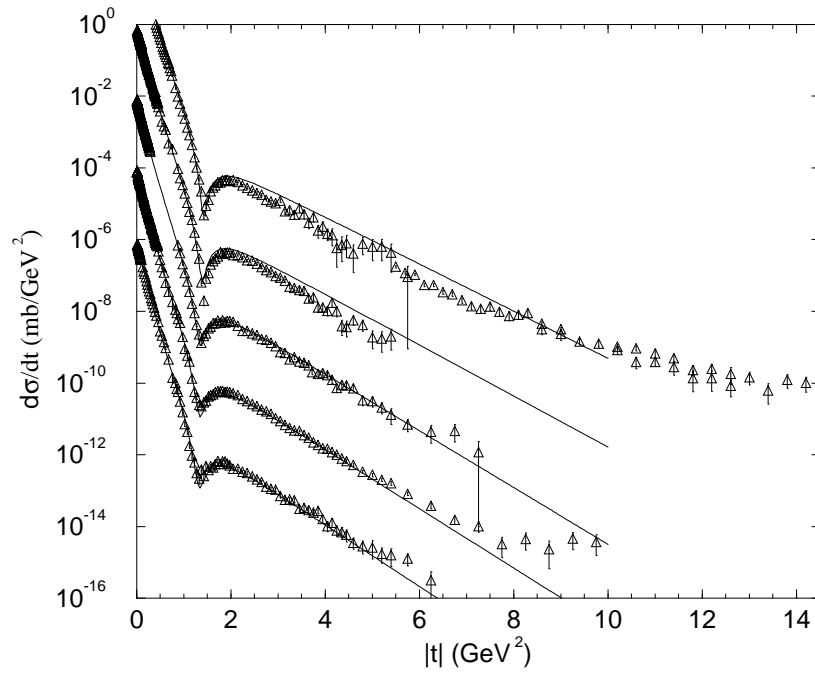


FIG. 3: The differential cross section obtained in this work taking into account the spin-flip amplitude, Eq. (6). The highest set of data corresponds to 23.5 and 27.4 GeV grouped together. The other sets (multiplied by powers of  $10^{-2}$ ) are 30.5, 44.6, 52.8, and 62 GeV.



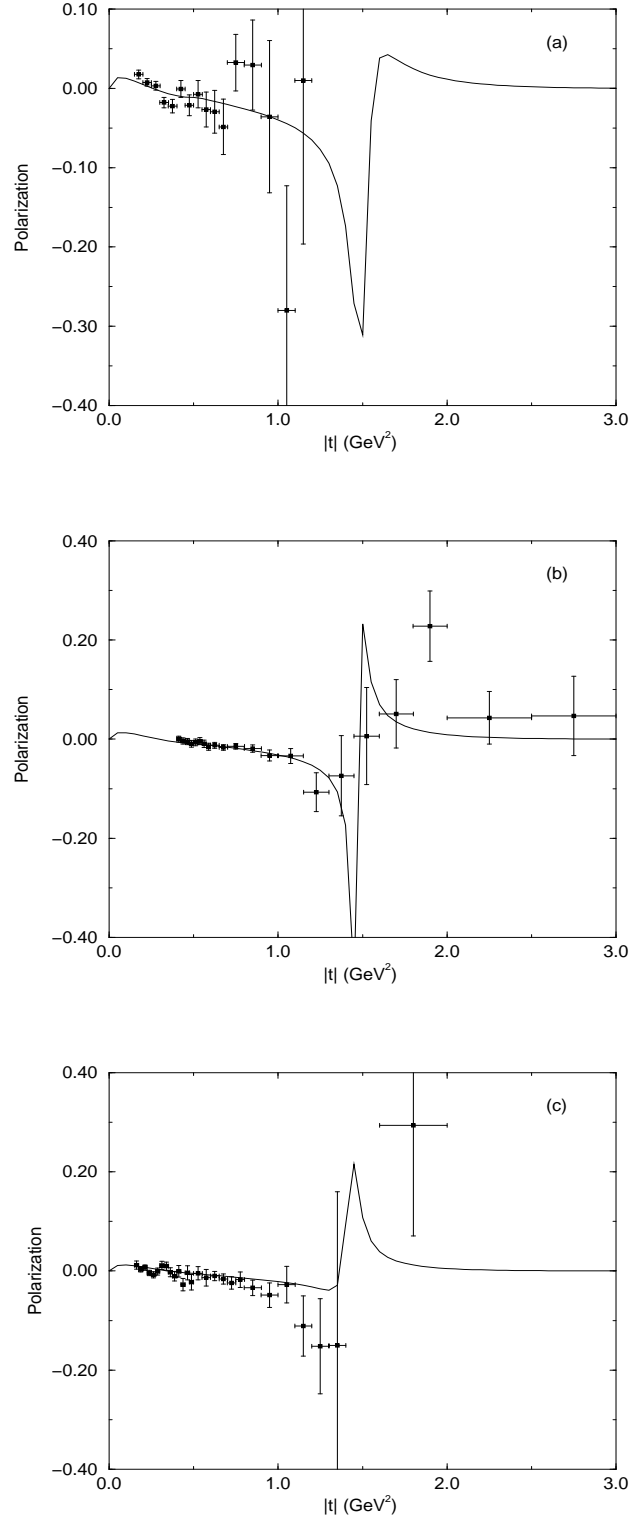


FIG. 4: Results from fitting polarization data at (a) 13.8 GeV, (b) 16.8 GeV, and (c) 23.8 GeV (see Table II).

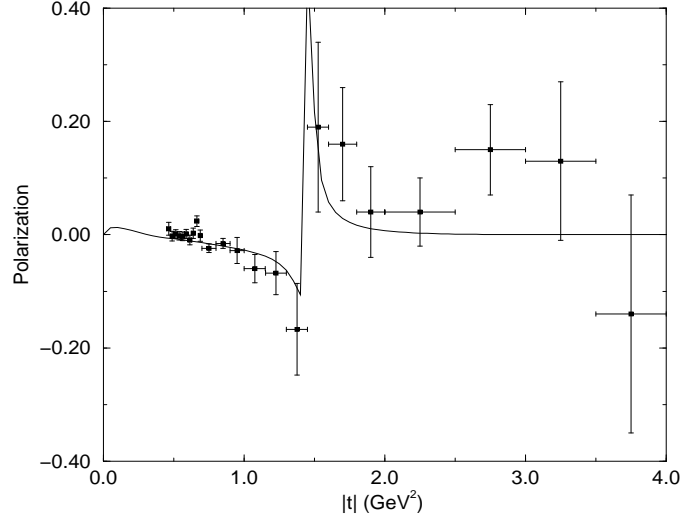


FIG. 5: The prediction for the polarization at 19.4 GeV (not used in the fit) compared with the experimental data at that energy (parameters from Table II).

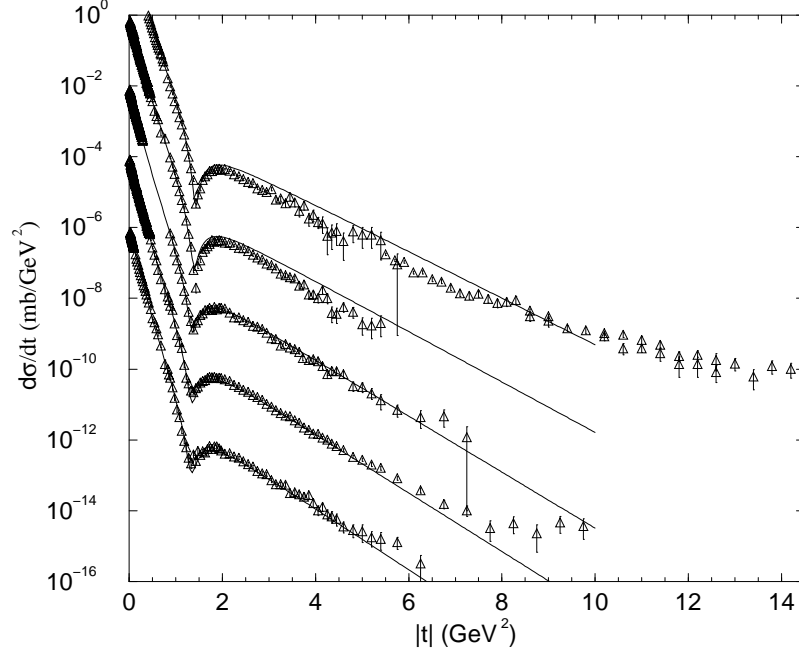


FIG. 6: The differential cross section obtained in this work taking into account the spin-flip amplitude through Eq. (8). About the data see Fig. 3.

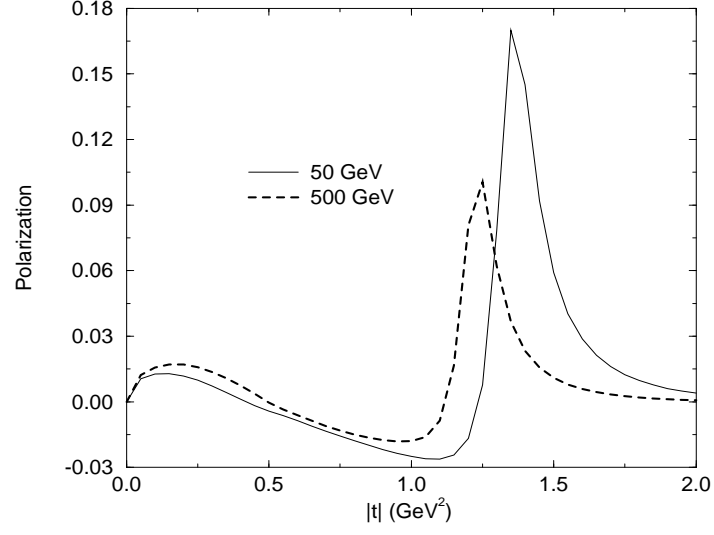


FIG. 7: The polarization predictions for  $\sqrt{s} = 50$  and 500 GeV with the parameters of Table I.

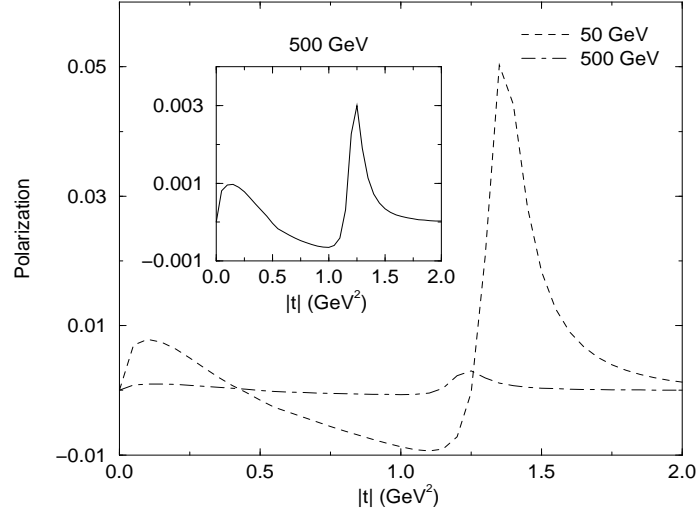


FIG. 8: The polarization predictions for 50 and 500 GeV with a detailed view of the data at 500 GeV in the inset (parameters from Table II).